

Nanocompatible Chemistry toward Fabrication of Target-Specific Gold Nanoparticles

Raghuraman Kannan,* Valerie Rahing, Cathy Cutler, Ravi Pandrapragada, Kavita K. Katti, Vijaya Kattumuri, J. David Robertson, Stan J. Casteel, Silvia Jurisson, Charles Smith, Evan Boote, and Kattesh V. Katti*

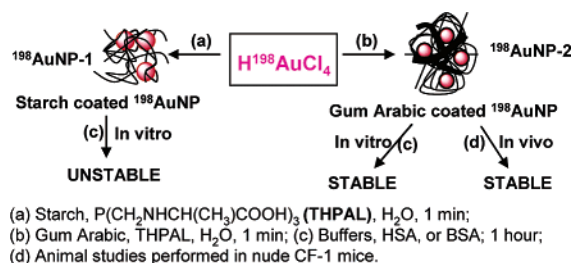
Departments of Radiology, Chemistry, and Physics, 301, Business loop 70W, Alton Bldg Laboratories, University of Missouri—Columbia, Columbia, Missouri 65212

Received May 10, 2006; E-mail: kannanr@health.missouri.edu; kattik@health.missouri.edu

Fundamental research encompassing chemistry in nanoscience/nanotechnology as they relate to achieving new developments in biomedicine is important because nanomedicine has the realistic potential to bring a paradigm shift in the way deadly diseases in humans are diagnosed and treated.¹ Unlike traditional medicine, nanomedicine utilizes nanoparticles as drugs with sizes similar to or smaller than that of cellular components for the detection or treatment of a variety of diseases.^{1,2} Development of new approaches for the synthesis of radioactive nanoparticles is of paramount importance as each nanoparticle will provide thousands of atoms with destructive power to kill cancer cells.³ For example, nanosized β -emitting gold [Au-198 ($\beta_{\text{max}} = 0.96$ MeV; $t_{1/2} = 2.7$ days) and Au-199 ($\beta_{\text{max}} = 0.46$ MeV; $t_{1/2} = 3.14$ days)] consist of at least 20000 atoms of β -emitters, which could deliver a lethal destructive pay load with enormous power to eradicate or control specific tumors. Therefore, radioactive nanoparticles can inherently carry a higher destructive pay load than traditional therapeutic pharmaceuticals.³ Conventional synthetic strategies (e.g., reduction via NaBH_4 or citrate) for the production of gold nanoparticles (AuNPs) do not yield desirable results when applied toward the production of radioactive AuNPs at tracer levels which employ very low concentrations of substrates. Therefore, development of novel chemistry that is compatible at nanoscale levels is imperative for achieving innovative advances in nanoscience and nanotechnology. Indeed, generation of nanoparticulate Au-198/199, under clinical settings, using solution-based nontoxic reducing agents in the presence of target-specific biomolecular matrices is still a major challenge.^{3c,d} As part of our ongoing research efforts in the design and development of cancer diagnostic/therapeutic radiopharmaceuticals,⁴ we, herein, report an efficient synthetic methodology with practical implications for the generation of $^{198}\text{AuNPs}$. We also report, herein, the “proof-of-principle” on the organ-specific localization capabilities of therapeutic $^{198}\text{AuNPs}$ in small animal models. Our approach toward the fabrication of biocompatible AuNPs is very unique in several ways, for example: (i) the application of the nontoxic $\text{P}(\text{CH}_2\text{NHCH}(\text{CH}_3)\text{COOH})_3$ (THPAL)⁵ reducing agent provides an unprecedented pathway to produce gold nanoparticles at acidic pH; (ii) utilization of edible and nontoxic biologically benign matrices stabilizes $^{198}\text{AuNPs}$; and (iii) spontaneous generation of $^{198}\text{AuNPs}$ in aqueous media can be easily practiced under clinical conditions. Gold nanoparticles are traditionally synthesized via the reduction of AuCl_4^- with NaBH_4 or citrate. However, traditional hydridic and carboxylate-based reduction strategies cannot be extended to the production of $^{198}\text{AuNPs}$.

$^{198}\text{AuCl}_4^-$ as produced through irradiation experiments within the nuclear reactor is available at acidic pH in hydrochloric acid media. Reduction with NaBH_4 will not proceed in acidic medium; likewise, citric acid tends to protonate itself under acidic conditions,

Scheme 1. Synthesis of $^{198}\text{AuNPs}$ in Different Biomolecular Matrix



making it less desirable for reducing $^{198}\text{AuCl}_4^-$ to produce $^{198}\text{AuNPs}$. Therefore, more effective reducing agents that work under acidic pH with favorable kinetics for rapid reduction of radiometals at extreme low concentrations ($\sim 10^{-8}$ M) are needed for the production of radioactive $^{198}\text{AuNPs}$. To circumvent existing problems associated with the production of $^{198}\text{AuNPs}$, we have chosen trimeric alanine-based phosphine, $\text{P}(\text{CH}_2\text{NHCH}(\text{CH}_3)\text{COOH})_3$ (THPAL), as a reducing agent (Scheme 1).⁵ Figure 1 shows the TEM image of AuNP-2 in gum arabic matrix. THPAL was recently discovered in our laboratories,⁶ and it reduces $^{198}\text{Au}^{3+}$ ions under acidic conditions in aqueous media from $^{198}\text{AuCl}_4^-$ within 5 min, thus demonstrating excellent kinetic propensity as a reducing agent for the production of $^{198}\text{AuNPs}$.⁷ Simple mixing of THPAL with $^{198}\text{Au}^{3+}$ ions initiates the phosphane-mediated reduction process with simultaneous oxidation into phosphanoxide.⁷ Assistance of amino acid carboxylic groups in the reduction process is purely serendipitous. It is important to note that reactions of alanine or glycine with $^{198}\text{Au}^{3+}$ do not result in the formation of AuNPs. These results clearly demonstrate that the reduction pathway of THPAL presumably involves synergistic reduction of the trivalent phosphorus and three anionic acids conjugated to it. The yields of ^{198}Au nanoparticle labeled with gum arabic were $>98\%$ as established by size exclusion chromatographic methods.⁷

Our studies have further focused on the stabilization of AuNPs via biocompatible matrices. Two different matrices, starch and gum arabic, were chosen for the current study. The core structure of polymeric starch molecules contains hydrogen bonded amylopectin rings which are capable of folding around the nanoparticles and, thus, are expected to prevent the aggregation of $^{198}\text{AuNPs}$. We have tested the efficacy of the edible gum arabic (glycoprotein)⁸ toward stabilizing $^{198}\text{AuNPs}$. Indeed, our detailed investigations have confirmed that gum arabic serves as an excellent backbone for the stabilization of $^{198}\text{AuNPs}$.⁹

In vitro stability studies of $^{198}\text{AuNP-1}$ and $^{198}\text{AuNP-2}$ have clearly demonstrated that the saccharide and protein structures provide exceptional stability for periods of over 6 months.⁷ Addition of a 20% solution of NaCl or pH 7.0 phosphate buffer solutions to

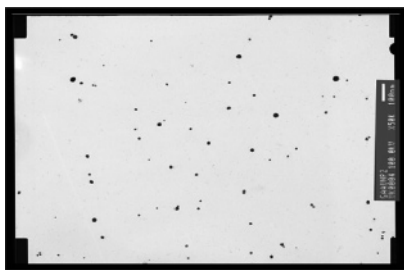


Figure 1. TEM image of the nonradioactive analogue of $^{198}\text{AuNP-2}$.

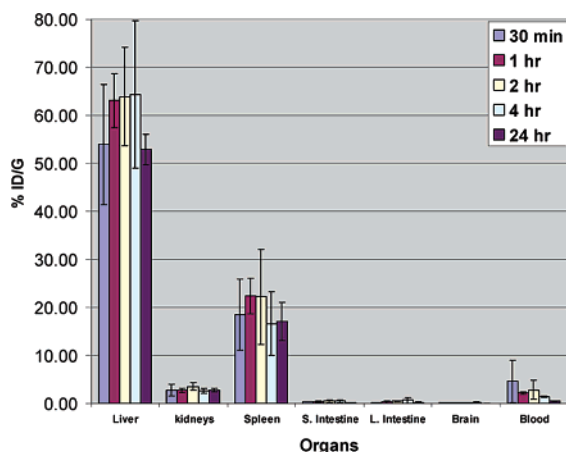


Figure 2. Biodistribution of $^{198}\text{AuNP-2}$ in nude CF-1 mice.

$^{198}\text{AuNP-2}$ did not cause any aggregation or decomposition of nanoparticles. Therefore, we have shown, for the first time, that readily injectable solutions of $^{198}\text{AuNPs}$ in saline or phosphate buffer solutions can be produced using AuNPs stabilized via gum arabic matrix. In sharp contrast, it should be pointed out that significant aggregation was noted when $^{198}\text{AuNP-1}$ was formulated in 20% saline or pH 7.0 phosphate buffer solutions. Therefore, we have selected $^{198}\text{AuNP-2}$ (gum arabic stabilized $^{198}\text{AuNPs}$) for further in vivo pharmacokinetic studies. The biodistribution studies of the $^{198}\text{AuNP-2}$ were performed in normal CF-1 mice. Pharmacokinetic studies indicate that a significant percentage (>85%) of $^{198}\text{AuNP-2}$ were localized in the liver (Figure 2). These pharmacokinetic studies clearly demonstrate that stabilization of gold nanoparticles using the biocompatible glycoprotein results in target-specific delivery of radioactive AuNPs to liver with minimal uptake by the nontarget organs.⁷ The significant accumulation of $^{198}\text{AuNP-2}$ in liver could deliver optimum destructive pay load for treatment of liver tumors. It is important to recognize that the target-specific destructive pay load of radioactive gold nanoparticles can be tuned to different organs and tumor sites.

Our results on the nanocompatible chemistry toward production, in vivo/in vitro stabilization, and target-specific delivery of gold

nanoparticles have culminated into a major advance toward readily injectable nanoparticulate vectors for potential applications in molecular imaging and therapy.

Acknowledgment. This work was supported by funds from the National Cancer Institute grant on Cancer Nanotechnology Platform No. 1R01CA119412-01.

Supporting Information Available: TEM images and size distribution histogram for starch and gum arabic stabilized gold nanoparticles. This material is available free of charge via the Internet at <http://pubs.acs.org>.

References

- (1) For recent progress in nanomedicine, see: (a) Barnard, S. A. *Nat. Mater.* **2006**, *5*, 245–248. (b) Peters, R. *Small* **2006**, *2*, 452–456. (c) Moghimi, S. M.; Hunter, A. C.; Murray, J. C. *FASEB J.* **2005**, *19*, 311–330. (d) Sridhar, S.; Amiji, M.; Shenoy, D.; Nagesha, D.; Weissig, V.; Fu, W. *Proc. SPIE-Int. Soc. Opt. Eng.* **2005**, *6008*, 600816/1–600816/8.
- (2) Selected references on the application of nanoparticles in disease detection and treatment: (a) Hansen, J. A.; Wang, J.; Kawde, A. N.; Xiang, Y.; Gothelf, K. V.; Collins, G. *J. Am. Chem. Soc.* **2006**, *128*, 2228–2229. (b) Huo, Q.; Liu, J.; Wang, L.-Q.; Jiang, Y.; Lambert, T. N.; Fang, E. *J. Am. Chem. Soc.* **2006**, *128*, 6447–6453. (c) Michalet, X.; Pinaud, F. F.; Bentolila, L. A.; Tsay, J. M.; Doose, S.; Li, J. J.; Sundaresan, G.; Wu, A. M.; Gambhir, S. S.; Weiss, S. *Science* **2005**, *307*, 538–544. (d) Georganopoulou, D. G.; Chang, L.; Nam, J. M.; Thaxton, C. S.; Mufson, E. J.; Klein, W. L.; Mirkin, C. A. *Proc. Natl. Acad. Sci. U.S.A.* **2005**, *102*, 2273–2276. (e) Sokolov, K.; Follen, M.; Aaron, J.; Pavlova, I.; Malpica, A.; Lotan, R.; Richards-Kortum, R. *Cancer Res.* **2003**, *63*, 1999–2004.
- (3) For references on nanoparticulate vectors for tumor detection and therapy, see: (a) Kukowska-Latallo, J. F.; Candido, K. A.; Cao, Z.; Nigavekar, S. S.; Majoros, I. J.; Thomas, T. P.; Balogh, L. P.; Khan, M. K.; Baker, J. R., Jr. *Cancer Res.* **2005**, *65*, 5317–5324. (b) Bielinska, A.; Eichman, J. D.; Lee, I.; Baker, J. R., Jr.; Balogh, L. J. *Nano. Res.* **2002**, *4*, 395–403. (c) Balogh, L. P.; Nigavekar, S. S.; Cook, A. C.; Minc, L.; Khan, M. K. *PharmaChem* **2003**, *2*, 94–99. (d) Balogh, L. P.; Nigavekar, S. S.; Sung, L. Y.; Balogh, P.; Shi, X. Y.; Cook, A. T.; Minc, L. D.; Khan, M. K. *J. Nucl. Med.* **2003**, *44*, 305–306. (e) Hainfeld, J. F.; Slatkin, D. N.; Smilowitz, H. M. *Phys. Med. Biol.* **2004**, *49*, N309–N315. (f) Harris, T. J.; von Maltzahn, G.; Derfus, A. M.; Ruoslahti, E.; Bhatia, S. N. *Angew. Chem., Int. Ed.* **2006**, *45*, 3161–3165.
- (4) (a) Pillarsetty, N.; Raghuraman, K.; Barnes, C. L.; Katti, K. V. *J. Am. Chem. Soc.* **2005**, *127*, 331–336. (b) Pillarsetty, N.; Katti, K. K.; Hoffman, T. J.; Volkert, W. A.; Katti, K. V.; Kamei, H.; Koide, T. *J. Med. Chem.* **2003**, *46*, 1130–1132. (c) Raghuraman, K.; Pillarsetty, N.; Volkert, W. A.; Barnes, C.; Jurisson, S.; Katti, K. V. *J. Am. Chem. Soc.* **2002**, *124*, 7276–7277.
- (5) THPAL has been found to be nontoxic in pigs at 50–100 mg/Kg of body weight.
- (6) Raghuraman, K.; Katti, K. K.; Barbour, L. J.; Pillarsetty, N.; Barnes, C. L.; Katti, K. V. *J. Am. Chem. Soc.* **2003**, *125*, 6955–6961.
- (7) See Supporting Information for complete details.
- (8) (a) Williams, P. A.; Idris, O. H. M.; Phillips, G. O. In *Handbook of Dietary Fiber*; Cho, S. S., Dreher, M. L., Eds.; Marcel Dekker: New York, 2001; pp 675–693. (b) Osman, M. E.; Williams, P. A.; Menzies, A. R.; Phillips, G. O. *J. Agric. Food Chem.* **1993**, *41*, 71–77.
- (9) Solutions were evaluated by UV–vis spectrophotometry to confirm the formation of AuNPs. The color change from pale yellow to purple was associated with a plasmon absorption band around 540 nm for $^{198}\text{AuNP-1}$ or $^{198}\text{AuNP-2}$ characteristic of nanoparticulate gold formation. To demonstrate internal consistency, nonradioactive analogues AuNP-1 and AuNP-2 were synthesized from HAuCl_4 (in 0.05 N HCl) using protocols similar to those used for synthesizing radioactive nanoparticles. UV–visible absorption spectra of AuNP-1 and AuNP-2 are identical to those of $^{198}\text{AuNP-1}$ and $^{198}\text{AuNP-2}$. TEM images of AuNP-1 and AuNP-2 were recorded, and the size distribution studies were performed.⁷

JA063280C